Structure functions for inclusive and diffractive DIS at future EICs [1]

Dagmar Bendova
Czech Technical University in Prague
Faculty of Nuclear Sciences and Physical Engineering

in collaboration with M. Matas, J. Cepila, J. G. Contreras, and V. P. Goncalves

Initial Stages 2021

11^{th} January, 2021

[1] Based on: Phys. Rev. D 100, 054015; Phys. Rev. C 102, 044318; arXiv:2009.14002

- How does the QCD structure of hadrons evolve with increasing energy?

- How does the QCD structure of hadrons evolve with increasing energy?

- How does the structure of a free proton change when it's bound inside a nucleus?

- $\gamma^* p$ cross section

$$\sigma_{T,L}^{\gamma^* p}(x, Q^2) = \sum_f \int \mathrm{d}^2 r \int \mathrm{d}z |\Psi^* \Psi|_{T,L}^f \sigma_{q\bar{q}}(\tilde{x}, \vec{r})$$

- Dipole-target cross section

$$\sigma_{q\bar{q}}(x, \vec{r}) = 2 \int \mathrm{d}^2 b \, N \left(x, \vec{r}, \vec{b}\right)$$

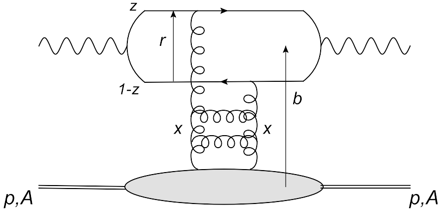

- Structure function F_2

$$F_2(x, Q^2) = \frac{Q^2}{4\pi^2 \alpha} \left(\sigma_T^{\gamma^* p} + \sigma_L^{\gamma^* p}\right)$$

- Diffractive structure function $F_2^{D(3)}$

$$F_2^{D(3)}(Q^2, \beta, x_{\mathbb{P}}) = F^D_{q\bar{q},L} + F^D_{q\bar{q},T} + F^D_{q\bar{q}g,T}$$

$$x_{\mathbb{P}} = \frac{Q^2 + M_X^2}{Q^2 + W^2}; \qquad \beta = \frac{Q^2}{Q^2 + M_X^2}; \qquad x = \beta x_{\mathbb{P}}$$

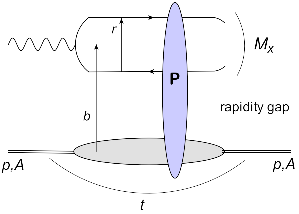

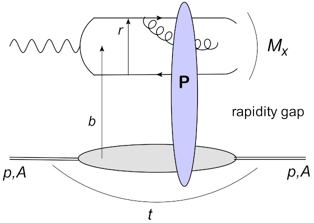

Diffractive DIS

- Diffractive structure function $F_2^{D(3)}$

$$F_2^{D(3)}(Q^2, \beta, x_{\mathbb{P}}) = F^D_{q\bar{q},L} + F^D_{q\bar{q},T} + F^D_{q\bar{q}g,T}$$

$$x_{\mathbb{P}} = \frac{Q^2 + M_X^2}{Q^2 + W^2}; \qquad \beta = \frac{Q^2}{Q^2 + M_X^2}; \qquad x = \beta x_{\mathbb{P}}$$

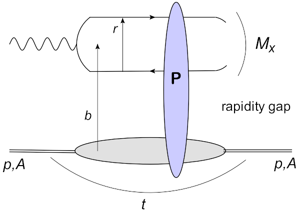

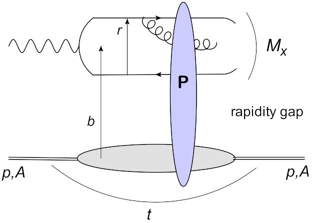

- $F_2^{D(3)}(Q^2, \beta, x_{\mathbb{P}})$ has a different sensitivity to the dipole-target amplitude (especially in the gluon part) than the inclusive F_2

- BK phenomenology has been successful in description of inclusive observables using the Ansatz

$$N\left(x, \vec{r}, \vec{b}\right) \to N(x, r)$$

- We are interested in the next step of the full $N\left(x, \vec{r}, \vec{b}\right)$ evolution

$$N\left(x, \vec{r}, \vec{b}\right) \to N(x, r, b)$$

Balitsky–Kovchegov evolution equation (at LO)

- Evolution of the scattering amplitude N of a $q\bar{q}$ dipole off a hadronic target.

  $\rightarrow$ Dynamical balance between the gluon emission and recombination.

$$\frac{\partial N(r_{xy}, b_{xy}, Y)}{\partial Y} = \int \mathrm{d}\vec{r}_{xz} K(r_{xy}, r_{xz}, r_{zy}) \Big[N(r_{xz}, b_{xz}, Y) + N(r_{zy}, b_{zy}, Y) - N(r_{xy}, b_{xy}, Y) - N(r_{xz}, b_{xz}, Y) N(r_{zy}, b_{zy}, Y) \Big]$$

- Dipole and the target hadron are interconnected

  $\rightarrow$ evolution of the dipole structure gives information about target structure

Evolution kernel

- Describes the probability of a gluon emission.
- Different approximations of the calculation lead to several forms of kernels

Evolution kernel

- Describes the probability of a gluon emission.
- Different approximations of the calculation lead to several forms of kernels
- **Running coupling kernel** [2]

$$K^{rc}(r, r_1, r_2) = \frac{\alpha_S(r^2)N_C}{2\pi^2}\left[\frac{r^2}{r_1^2 r_2^2} + \frac{1}{r_1^2}\left(\frac{\alpha_S(r_1^2)}{\alpha_S(r_2^2)} - 1\right) + \frac{1}{r_2^2}\left(\frac{\alpha_S(r_2^2)}{\alpha_S(r_1^2)} - 1\right)\right]$$

[2] I. Balitsky, Phys. Rev. D 75 (2007) 014001

Evolution kernel

- Describes the probability of a gluon emission.
- Different approximations of the calculation lead to several forms of kernels
- **Running coupling kernel** [2]

$$K^{rc}(r, r_1, r_2) = \frac{\alpha_S(r^2)N_C}{2\pi^2}\left[\frac{r^2}{r_1^2 r_2^2} + \frac{1}{r_1^2}\left(\frac{\alpha_S(r_1^2)}{\alpha_S(r_2^2)} - 1\right) + \frac{1}{r_2^2}\left(\frac{\alpha_S(r_2^2)}{\alpha_S(r_1^2)} - 1\right)\right]$$

- **Collinearly improved kernel** [3]

$$K^{ci}(r, r_1, r_2) = \frac{\bar{\alpha}_S}{2\pi}\frac{r^2}{r_1^2 r_2^2}\left[\frac{r^2}{\min(r_1^2, r_2^2)}\right]^{\pm\bar{\alpha}_S A_1} K_{DLA}\left(\sqrt{L_{r_1 r} L_{r_2 r}}\right)$$

$$K_{DLA}(\rho) = \frac{J_1(2\sqrt{\bar{\alpha}_S \rho^2})}{\sqrt{\bar{\alpha}_S \rho^2}}, \qquad L_{r_i,r} = \ln\left(\frac{r_i^2}{r^2}\right)$$

[2] I. Balitsky, Phys. Rev. D 75 (2007) 014001

[3] E. Iancu et al., Phys. Lett. B 750 (2015) 643; A. Sabio Vera, Nucl. Phys. B722 (2005) 65

Implementation of impact-parameter dependence

- The equation is solved using a new initial condition that takes into account the location of the end-points of the dipole

$$N(\vec{r}, \vec{b}, Y = 0) = 1 - \exp\left[-\frac{1}{2}\frac{Q_S^2}{4} r^2 T(\vec{b}_{q_1}, \vec{b}_{q_2})\right]$$

$$T(\vec{b}_{q_1}, \vec{b}_{q_2}) = \exp\left(-\frac{b_{q_1}^2}{2B}\right) + \exp\left(-\frac{b_{q_2}^2}{2B}\right)$$

Implementation of impact-parameter dependence

- The equation is solved using a new initial condition that takes into account the location of the end-points of the dipole

$$N(\vec{r}, \vec{b}, Y=0) = 1 - \exp\left[-\frac{1}{2}\frac{Q_S^2}{4} r^2 T(\vec{b}_{q_1}, \vec{b}_{q_2})\right]$$

$$T(\vec{b}_{q_1}, \vec{b}_{q_2}) = \exp\left(-\frac{b_{q_1}^2}{2B}\right) + \exp\left(-\frac{b_{q_2}^2}{2B}\right)$$

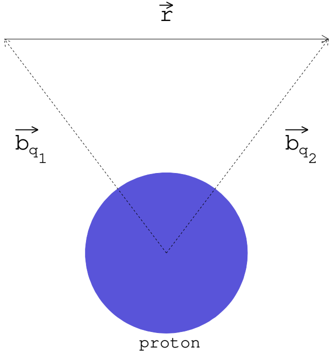

- The r behavior mimics the models for the b-independent dipole amplitude.
- The b behavior contains an exponential fall-off for dipole-ends far away from the target.

The problem of Coulomb tails

- Evolution with an exponentially falling initial condition and K^{rc} (*dashed lines*) increases the contribution at large impact parameters into a power-like growth.
  - Complications for phenomenological applications.
- Evolution at high-b can be suppressed by suppressing large daughter dipoles.

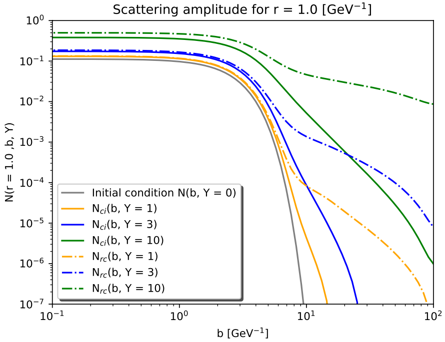

J. Cepila, J. G. Contreras, M. Matas; Phys. Rev. D 99, 051502

The problem of Coulomb tails

- Evolution with an exponentially falling initial condition and K^{rc} (*dashed lines*) increases the contribution at large impact parameters into a power-like growth.
  - Complications for phenomenological applications.
- Evolution at high-b can be suppressed by suppressing large daughter dipoles.

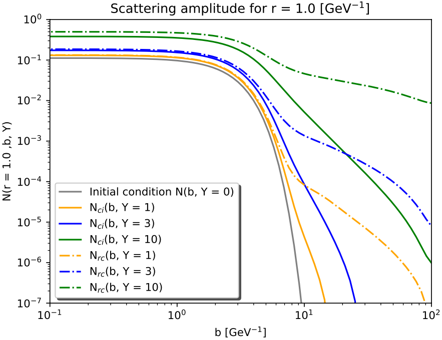

J. Cepila, J. G. Contreras, M. Matas; Phys. Rev. D 99, 051502

- Using the collinearly improved kernel K^{ci}(*full lines*)
  - Large daughter dipoles are suppressed as a result of time-ordering of the emissions.
  - Suppression by several orders of magnitude at large b.

- **Glauber–Gribov approach (b-BK-GG)**
  - Solution of the b-BK for proton target coupled to Glauber–Gribov prescription

$$N^{A}_{\mathrm{GG}}(r_{xy}, b_{xy}, Y) = \left[1 - \exp\left(-\frac{1}{2} T_A(b_{xy}) \sigma_{q\bar{q}}(Y, r_{xy})\right)\right]$$

$$\sigma_{q\bar{q}}(Y, r_{xy}) = \int \mathrm{d}^2 b \, 2N^{p}(r_{xy}, b_{xy}, Y)$$

  - Nuclear thickness function $T_A(b_{xy})$ obtained from a Woods–Saxon distribution
  - Approach followed in other studies, however the compatibility of BK + GG not clear

Modification of b-BK to the nuclear case

- **Glauber–Gribov approach (b-BK-GG)**
  - Solution of the b-BK for proton target coupled to Glauber–Gribov prescription

$$N^A_{\mathrm{GG}}(r_{xy}, b_{xy}, Y) = \left[1 - \exp\left(-\frac{1}{2}T_A(b_{xy})\sigma_{q\bar{q}}(Y, r_{xy})\right)\right]$$

$$\sigma_{q\bar{q}}(Y, r_{xy}) = \int \mathrm{d}^2 b\, 2N^p(r_{xy}, b_{xy}, Y)$$

  - Nuclear thickness function $T_A(b_{xy})$ obtained from a Woods–Saxon distribution
  - Approach followed in other studies, however the compatibility of BK + GG not clear
- **Nuclear BK evolution (b-BK-A)**
  - The initial condition represents a specific nucleus

$$N^A(r_{xy}, b_{xy}, Y = 0) = 1 - \exp\left[-\frac{1}{2}\frac{Q^2_{s_0}(A)}{4}\, r^2_{xy}\, T_A\left(b_{q_1}, b_{q_2}\right)\right]$$

$$T_A\left(b_{q_1}, b_{q_2}\right) = k\left[T_A(b_{q_1}) + T_A(b_{q_2})\right]$$

  $\rightarrow$ $T_A(b_{q_i})$ uses the Woods–Saxon distribution
  - Initial nuclear saturation scale $Q^2_{s_0}(A)$ obtained from the comparison of nuclear F_2 at the initial condition to EPPS16 predictions.

Predictions for proton and nuclear structure functions

using the b-dependent Balitsky–Kovchegov equation

- Good agreement with the data measured at HERA[4].
- Results obtained without any additional ad-hoc terms (or parameters) needed to describe the data correctly.

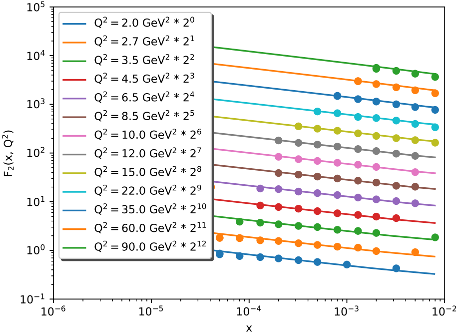

DB, J. Cepila, J. G. Contreras, M. Matas; Phys. Rev. D 100, 054015

[4] H1, ZEUS: JHEP 01 (2010) 109.

- A sizeable difference between the b-BK-GG and b-BK-A approaches
  $\rightarrow$ the difference clearly depends on x, Q^2, and also A

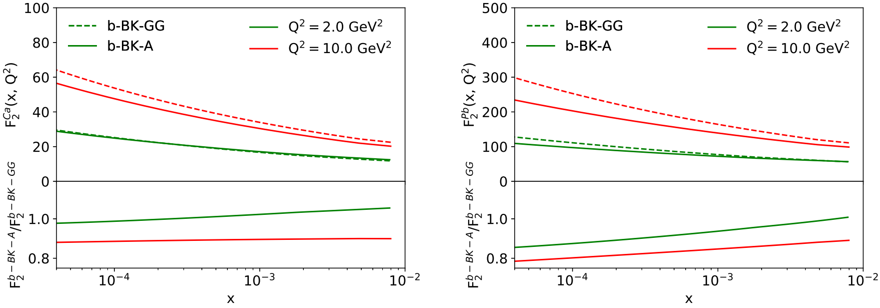

J. Cepila, J. G. Contreras, M. Matas; Phys. Rev. C 102 (2020) 044318

- A reasonable agreement with the HERA data on the diffractive reduced cross section.
- Results obtained with b-BK amplitudes predict smaller proton $F_2^{D(3)}$ compared to other models.

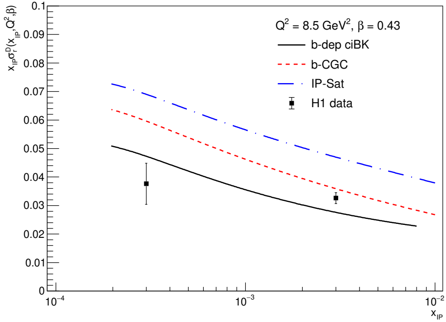

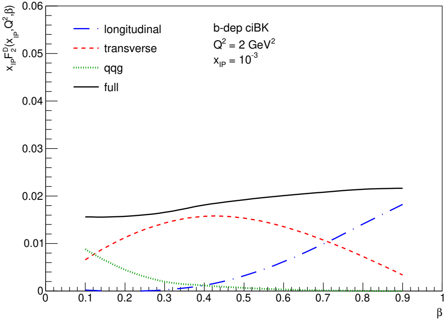

DB, J. Cepila, J. G. Contreras, V.P. Goncalves, M. Matas; arXiv:2009.14002

Diffractive DIS: nuclear structure functions

- Results of the b-BK-A approach are shown for Ca and Pb at low Q^2 and large β
- F_2^D ratio slightly larger for heavier nuclei
- $q\bar{q}g$ component (*green line*) strongly suppressed at larger A.

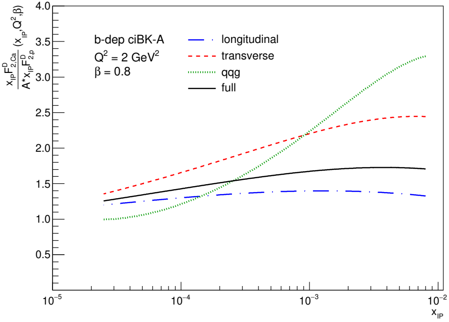

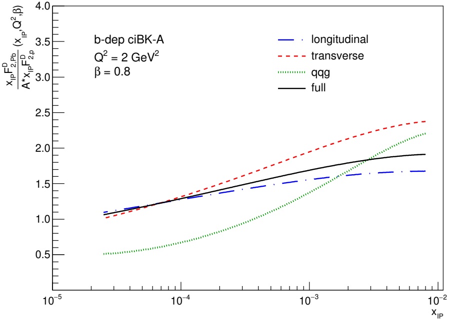

DB, J. Cepila, J. G. Contreras, V.P. Goncalves, M. Matas; arXiv:2009.14002

Conclusions

- The collinearly improved kernel suppresses the Coulomb tails.

[5] DB, J. Cepila, J. G. Contreras, M. Matas: Phys. Rev. D 100, 054015; arXiv:2006.12980

Conclusions

- The collinearly improved kernel suppresses the Coulomb tails.
- Solutions to the b-BK equation obtained for proton and nuclear targets.

[5] DB, J. Cepila, J. G. Contreras, M. Matas: Phys. Rev. D 100, 054015; arXiv:2006.12980

Conclusions

- The collinearly improved kernel suppresses the Coulomb tails.
- Solutions to the b-BK equation obtained for proton and nuclear targets.
- Successful application of dipole amplitudes obtained by solving b-BK into several QCD processes

[5] DB, J. Cepila, J. G. Contreras, M. Matas: Phys. Rev. D 100, 054015; arXiv:2006.12980

- The collinearly improved kernel suppresses the Coulomb tails.
- Solutions to the b-BK equation obtained for proton and nuclear targets.
- Successful application of dipole amplitudes obtained by solving b-BK into several QCD processes
  - **Proton and nuclear structure functions**

[5] DB, J. Cepila, J. G. Contreras, M. Matas: Phys. Rev. D 100, 054015; arXiv:2006.12980

Conclusions

- The collinearly improved kernel suppresses the Coulomb tails.
- Solutions to the b-BK equation obtained for proton and nuclear targets.
- Successful application of dipole amplitudes obtained by solving b-BK into several QCD processes
  - **Proton and nuclear structure functions**
  - **Diffractive DIS with protons and nuclei**

[5] DB, J. Cepila, J. G. Contreras, M. Matas: Phys. Rev. D 100, 054015; arXiv:2006.12980

Conclusions

- The collinearly improved kernel suppresses the Coulomb tails.
- Solutions to the b-BK equation obtained for proton and nuclear targets.
- Successful application of dipole amplitudes obtained by solving b-BK into several QCD processes
  - **Proton and nuclear structure functions**
  - **Diffractive DIS with protons and nuclei**
  - Other processes, e.g. vector meson production[5] (see backup)

[5] DB, J. Cepila, J. G. Contreras, M. Matas: Phys. Rev. D 100, 054015; arXiv:2006.12980

Conclusions

- The collinearly improved kernel suppresses the Coulomb tails.
- Solutions to the b-BK equation obtained for proton and nuclear targets.
- Successful application of dipole amplitudes obtained by solving b-BK into several QCD processes
  - **Proton and nuclear structure functions**
  - **Diffractive DIS with protons and nuclei**
  - Other processes, e.g. vector meson production[5] (see backup)
- Presented results are of an interest for measurements at current and future facilities such as LHC, EIC or LHeC.

[5] DB, J. Cepila, J. G. Contreras, M. Matas: Phys. Rev. D 100, 054015; arXiv:2006.12980

BACKUP SLIDES

Production of vector mesons

- The approach is also applicable to production of vector mesons off protons and nuclei.

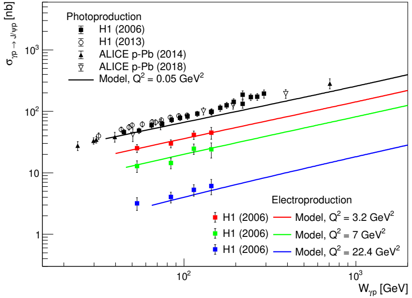

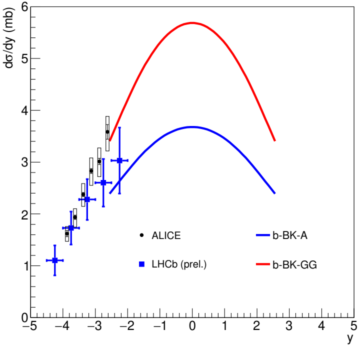

DB, J. Cepila, J. G. Contreras, M. Matas; Phys. Rev. D 100, 054015; arXiv:2006.12980

Influence of the individual collinear kernel terms on the Coulomb tails

$$K_{ci}^1 = \frac{\bar{\alpha}_S}{2\pi}\frac{r^2}{r_1^2 r_2^2}; \qquad K_{ci}^2 = \left[\frac{r^2}{\min(r_1^2, r_2^2)}\right]^{\pm\bar{\alpha}_S A_1}; \qquad K_{ci}^3 = K_{DLA}\left(\sqrt{L_{r_1 r} L_{r_2 r}}\right)$$

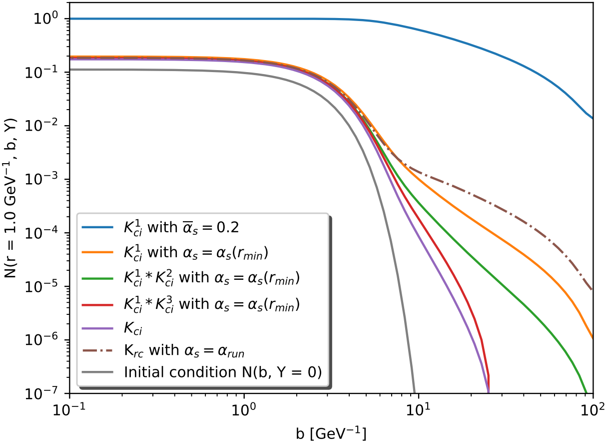

Comparison of dipole-nucleus scattering amplitudes

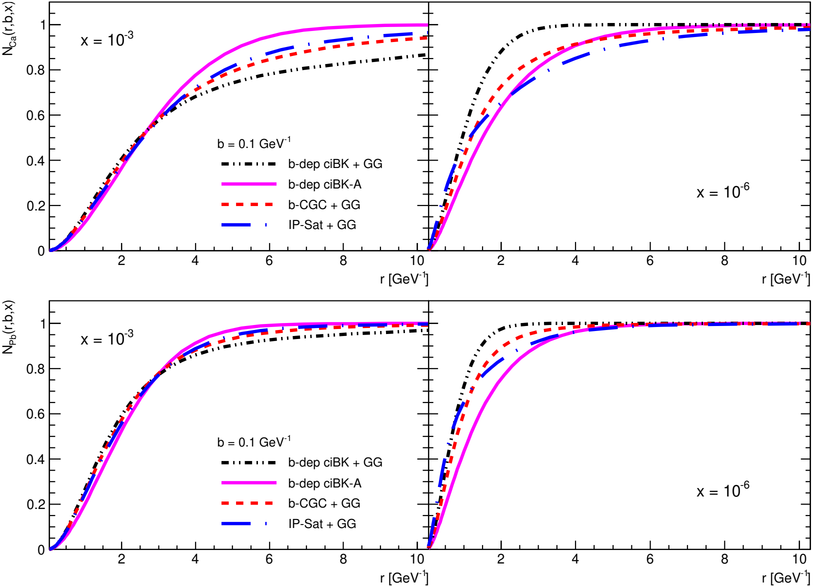

Nuclear saturation scale

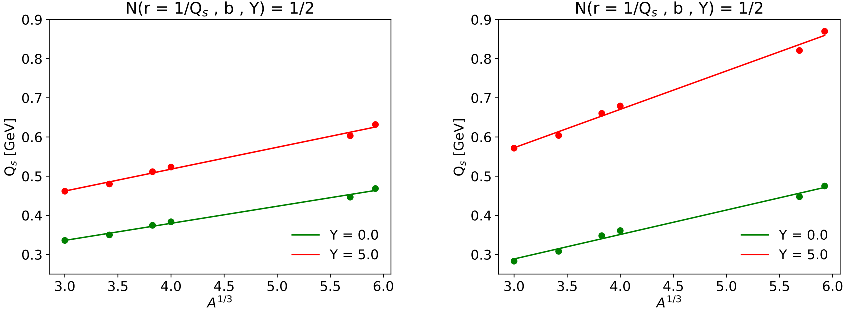

Figure: Saturation scale at two different rapidities for an impact parameter $b = 0.01\ \mathrm{GeV}^{-1}$ for the b-BK-A (left) and b-BK-GG (right) approaches. The solid bullets are the results from the evolution and are well described by a linear function.

Nuclear suppresion factors

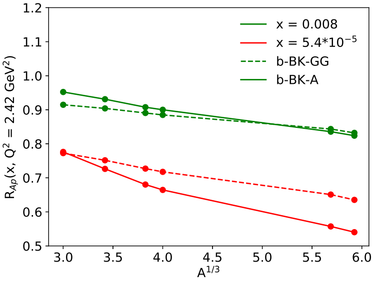

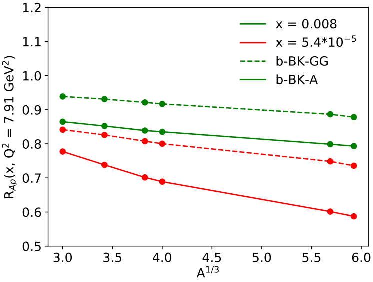

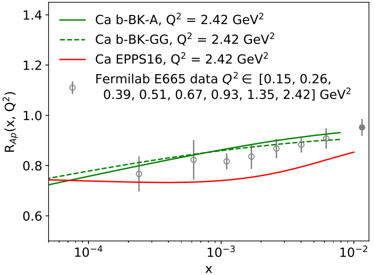

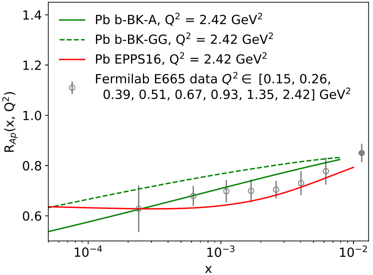

- Diffractive DIS cross section

$$\frac{\mathrm{d}\sigma^{eh\to eXh}}{\mathrm{d}\beta\mathrm{d}Q^2\mathrm{d}x_{\mathbb{P}}} = \frac{4\pi\alpha_{em}^2}{\beta Q^4}\left[1 - y + \frac{y^2}{2}\right]\left(F_2^{D(3)}(x_{\mathbb{P}}, \beta, Q^2) - \frac{y^2}{1+(1-y)^2}F_L^{D(3)}(x_{\mathbb{P}}, \beta, Q^2)\right)$$

- Diffractive structure function $F_2^{D(3)}$

$$F_2^{D(3)}(Q^2, \beta, x_{\mathbb{P}}) = F^D_{q\bar{q},L} + F^D_{q\bar{q},T} + F^D_{q\bar{q}g,T}$$

- New variables $x_{\mathbb{P}}$ and β

$$x_{\mathbb{P}} = \frac{Q^2 + M_X^2}{Q^2 + W^2}; \qquad \beta = \frac{Q^2}{Q^2 + M_X^2}; \qquad x = \beta x_{\mathbb{P}}$$

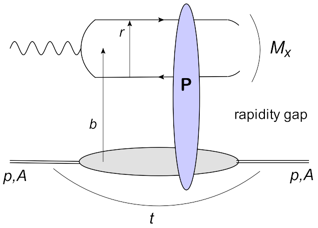

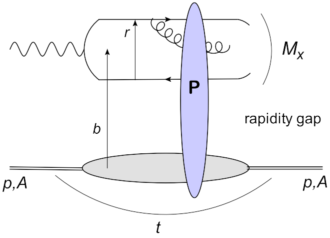

Diffractive DIS

- Longitudinal contribution to F_2^D

$$x_{\mathbb{P}} F^D_{q\bar{q},L}(x_{\mathbb{P}}, \beta, Q^2) = \frac{N_c Q^6}{4\pi^3 \beta} \sum_f e_f^2 \int_{z_0}^{1/2} \mathrm{d}z z^3 (1-z)^3 \Phi_0$$

- Transverse contribution

$$x_{\mathbb{P}} F^D_{q\bar{q},T}(x_{\mathbb{P}}, \beta, Q^2) = \frac{N_c Q^4}{16\pi^3 \beta} \sum_f e_f^2 \int_{z_0}^{1/2} \mathrm{d}z z(1-z) \left\{ \epsilon^2 [z^2 + (1-z)^2] \Phi_1 + m_f^2 \Phi_0 \right\}$$

- Auxiliary functions $\Phi_{0,1}$

$$\Phi_{0,1} = \int \mathrm{d}^2 b \left[\int_0^\infty \mathrm{d}r r K_{0,1}(\epsilon r) J_{0,1}(kr) \frac{\mathrm{d}\sigma_{q\bar{q}}}{\mathrm{d}^2 b}(b, r, x_{\mathbb{P}}) \right]^2$$

- Transverse $q\bar{q}g$ component

$$x_{\mathbb{P}} F^D_{q\bar{q}g,T}(x_{\mathbb{P}}, \beta, Q^2) = \frac{\alpha_s \beta}{8\pi^4} \sum_f e_f^2 \int \mathrm{d}^2 b \int_0^{Q^2} \mathrm{d}\kappa^2 \int_\beta^1 \mathrm{d}z \left\{ \kappa^4 \ln \frac{Q^2}{\kappa^2} \left[\left(1 - \frac{\beta}{z}\right)^2 + \left(\frac{\beta}{z}\right)^2 \right] \left[\int_0^\infty \mathrm{d}r r \frac{\mathrm{d}\sigma_g}{\mathrm{d}^2 b} K_2(\sqrt{z}\kappa r) J_2(\sqrt{1-z}\kappa r) \right]^2 \right\}$$

$$\frac{\mathrm{d}\sigma_g}{\mathrm{d}^2 b} = 2 \left[1 - \left(1 - \frac{1}{2} \frac{\mathrm{d}\sigma_{q\bar{q}}}{\mathrm{d}^2 b} \right)^2 \right]$$

Results for DDIS on protons with b-BK amplitudes

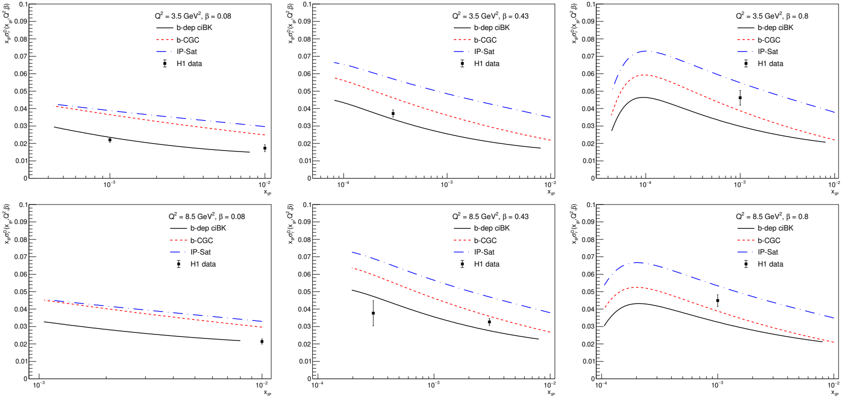

Diffractive DIS: nuclear structure functions – $x_{\mathbb{P}}$-dependence

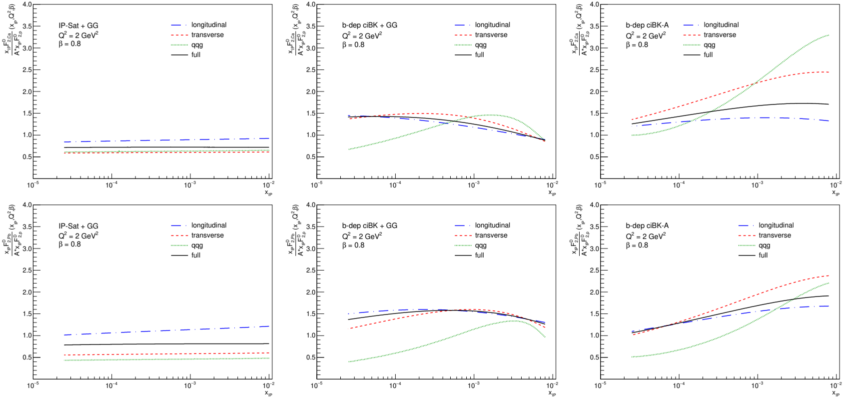

DB, J. Cepila, J. G. Contreras, V.P. Goncalves, M. Matas; arXiv:2009.14002

More results for DDIS with nuclei: β-dependence for the F_2^D ratio

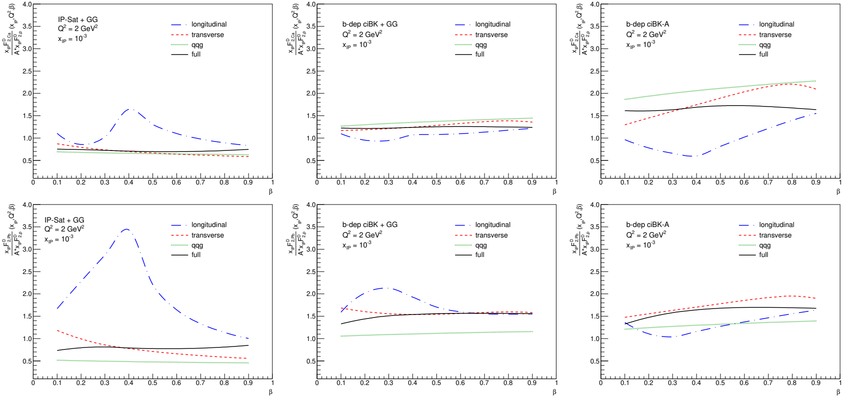

More results for nuclear DDIS: reduced cross section's ratio